DEVELOPMENT AND TEST OF A LARGE-APERTURE Nb_3Sn COS-THETA DIPOLE COIL WITH STRESS MANAGEMENT*

A.V. Zlobin†, M. Baldini, I. Novitski, D. Turrioni, E. Barzi, Fermilab, Batavia, IL 60510, USA

Abstract

A 123-mm aperture two-layer Nb_3Sn SMCT dipole coil has been developed at Fermilab to demonstrate and test the SMCT concept including coil design, fabrication technology and performance. The first SMCT coil was fabricated and assembled with 60-mm aperture Nb_3Sn coil inside a dipole mirror configuration and tested separately and in series with the insert coil. This paper summarizes the design, parameters, and quench performance of the large-aperture SMCT coil in a dipole mirror configuration.

MANUSCRIPTS

An innovative stress-management (SM) concept for cos-theta (CT) coils (SMCT coil concept) has been proposed at Fermilab [1], [2]. A large-aperture two-layer Nb_3Sn SMCT dipole coil was designed and manufactured to validate and test the SM concept including coil design, fabrication technology, and performance. The first large-aperture SMCT coil (SMCT1) was fabricated and assembled with a small-aperture Nb_3Sn coil inside a dipole mirror magnet.

SMCT1 coil tests in a dipole mirror structure was performed in two configurations - SMCTM1a with only powered two-layer SMCT1 coil and SMCTM1b with the SMCT coil connected in series with an inner two-layer dipole coil. The test goals are to prove the SMCT coil concept in two-layer and four-layer mirror configurations; demonstrate that the magnet can reach the targeted quench current at the established preload; study magnet training, training memory after thermal cycle, ramp rate and temperature dependences of the magnet quench current; and test the SMCT1 coil quench protection parameters.

This paper summarizes the SMCT1 coil design and parameters, the coil main fabrication steps, its assembly in the dipole mirror structure. The results of the SMCTM1a/b mirror test are also presented and discussed.

SMCT COIL DESIGN AND TEST CONFIGURATIONS

A cross-section and 3D view of the large-aperture SMCT1 dipole coil with transverse and longitudinal cuts at the coil non-lead end are shown in Fig. 1. The SMCT1 coil consists of two-layers. The turns in each layer are combined in 5 blocks wound into a stainless-steel structure with 5 mm radial and azimuthal block separation [3]. To produce a dipole field in the mag-net aperture, the number of turns in the blocks approximately follows the cos-theta distribution. The SMCT1 coil structure has a complex 3D geometry which requires using advanced Additive Manufacturing technologies. To produce accurate metallic SMCT1 coil parts, Direct Metal Laser Melting with stainless steel powder and CNC post-processing were used [4].

The coil uses a 15.1 mm wide and 1.319 mm (average) thick 40-strand Rutherford keystoned cable with a keystone angle of 0.805 degree. The cable is made of 0.7 mm diameter Nb_3Sn composite wire with a *Cu/nonCu* ratio of 1.13 and $J_c(15T;4.2K)$ of 1500 A/mm^2. The strand and cable cross-sections are also shown in Fig. 1. This cable was produced at Fermilab [5] and used in two-layer MBHSP dipoles developed for the LHC upgrades [6] and outer coils in the four-layer MDPCT1 [7] dipole.

Each coil block in its specific groove in both layers is surrounded with 0.5 mm thick ground insulation made of mica and S2-glass blanket. Consequently, azimuthal and radial components of the Lorentz force in each block are not accumulated but transmitted to the coil and magnet structures partially bypassing the coil blocks. The coil inner diameter is 123 mm, leaving ~0.5 mm of radial space for the coil radial insulation of the inner coil. The coil outer diameter is 206 mm. The details of the SMCT1 coil fabrication are reported in [3].

The SMCT1 coil was tested in a four-layer dipole mirror configuration using the MDPCT1 mechanical structure and two-layer inner MDP coil, which was originally developed and previously used as an inner coil in four-layer MDPCT1 dipole [7], [8]. The inner MDP and outer SMCT1 coils are separated by three layers of Kapton of total thickness of 0.3 mm. Two quench protection heaters, made of 0.025 mm thick stainless-steel strips etched on the 0.05 mm thick Kapton substrate, cover the four largest outer blocks of the SMCT1 coil. The heaters were placed between the first and the second layer of the four-layer ground insulation. Each layer thickness is 0.125 mm. The total Kapton thickness between the heater and the coil is 0.175 mm.

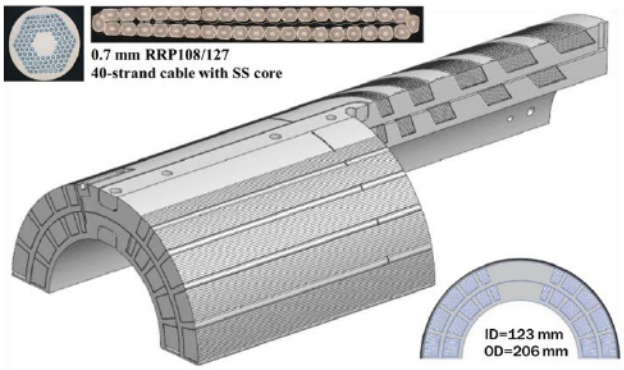

Figure 1: Nb_3Sn strand and cable cross-sections and 3D view of the large-aperture two-layer SMCT1 coil.

* Work supported by Fermi Research Alliance, LLC, under contract No. DE-AC02-07CH11359 with the U.S. DOE and by Jefferson Science Associates, LLC under contract No. DE-AC05-06OR23177
† zlobin@fnal.gov

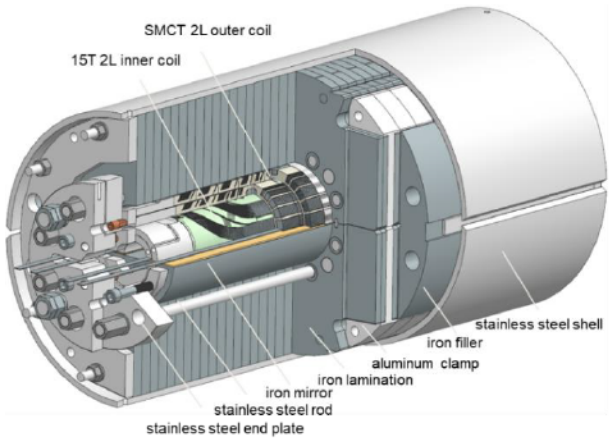

Figure 2: Four-layer mirror magnet design.

The coil assembly, surrounded by a 1-mm thick 316L stainless steel shell, was installed inside the bottom part of the horizontally split iron yoke. The yoke is made of AISI 1020 iron laminations with an outer diameter of 587 mm, connected by strong 7075-T6 Aluminum I-clamps, and enclosed in a 12.5-mm thick 316 stainless-steel skin.

The 3D view of the four-layer coil assembly in a dipole mirror structure is shown in Fig. 2. Coil ends are supported by two independent systems. The outer SMCT1 coil is supported by eight 24.5-mm diameter rods and 50 mm thick end plates. The inner coil is supported by four 30-mm diameter rods and 50 mm thick inside and 30 mm thick outside end plates (see Fig. 2).

The coil preload during assembly was applied by a combination of coil mid-plane, inter-coil, and coil-yoke radial shims; yoke-clamp interference; yoke-skin shims; and skin tension after welding. During magnet cool-down to the LHe temperatures, the coil stress is managed by the gap between the yoke blocks. After assembly the maximum stress in the inner MDP coil is less than 130 MPa and in the SMCT1 coil it is less than 50 MPa. After cooling-down the maximum stress in the inner MDP coil increases to ~175 MPa and in the SMCT1 coil to ~80 MPa.

SMCT1 COIL TEST

The mirror test was done in two configurations. First, the SMCT1 coil was powered independently (SMCTM1a configuration). Then it was connected and powered in series with the inner coil (SMCTM1b configuration). The calculated SMCT1 coil B_{max} limits at 1.9 K and 4.5 K in SMCTM1a are 14.2 T and 13.1 T reached at 16.5 kA and 14.8 kA respectively. SMCTM1b is limited by the inner MDP coil.

SMCTM1a test

The sequence of magnet test steps and coil quenches in SMCTM1a are shown in Fig. 3. SMCTM1a test started with magnet training (I) followed by quench current ramp rate studies (II) at 1.9 K and temperature dependence measurement (III) in the temperature range of 1.9-4.5 K. After thermal cycle (TC) to room temperature measurements of magnet training memory (IV), ramp rate (V) and temperature (VI) dependences were repeated at 1.9 K.

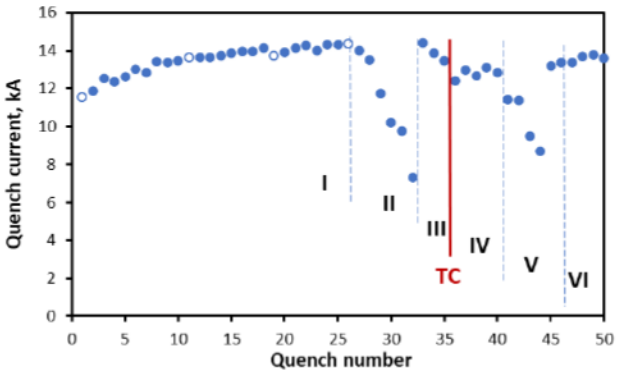

Figure 3: SMCTM1a test steps and quench sequence.

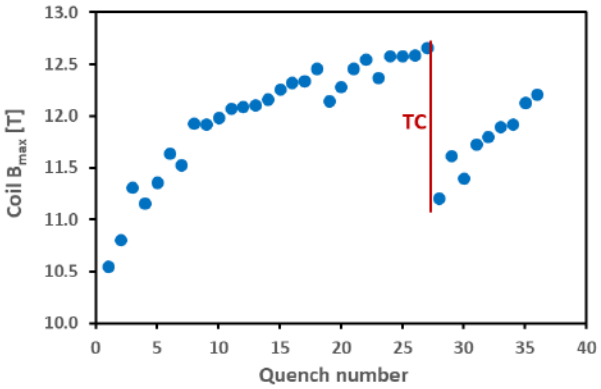

Figure 4: SMCT1 coil B_{max} vs. quench number at 20 A/s measured in SMCTM1a configuration at 1.9 K.

SMCTM1a training at 1.9 K is shown in Fig. 4. SMCT1 coil training started at coil B_{max} of 10.6 T which corresponds to 70% of the coil short sample limit at 1.9 K. After some training B_{max} in the SMCT1 coil of 12.7 T. All the quenches in SMCT1 coil were detected in the coil inner layer except the 1st quench that originated in the middle block 3, and 11th, 19th and 26th quenches which started in the pole block of the coil outer layer. Due to loss of voltage taps (VTs) on the coil inner-layer blocks the precise location of the quench origin in the inner layer was not possible. The 1st quench after TC was at 11.2 T which is higher than the first training quench. Thus, the magnet showed quit poor training memory with all the quenches in the coil inner layer. Due to slow training rate, magnet training was stopped after 9 training quenches. Magnet training before and after TC configuration was not completed.

Due to magnet long training before and after TC at 1.9 K, the coil degradation was estimated using the ramp rate and temperature dependences of the coil B_{max}, shown in Fig. 5 and Fig.6, and measured before and after TC.

The ramp rate dependence of the SMCT1 coil B_{max} shows linear reduction of the coil quench current with increasing current ramp rate. Such dependence indicates that AC losses in the cable are dominated by the hysteresis loss in the superconductor. The other two AC loss components, i.e., eddy current losses in strands and in cable, are relatively small. Linear extrapolation of the coil B_{max} to zero ramp rate gives a value of the maximum B_{max} value of 13.1 T which is 91% of the expected SSL at 1.9 K.

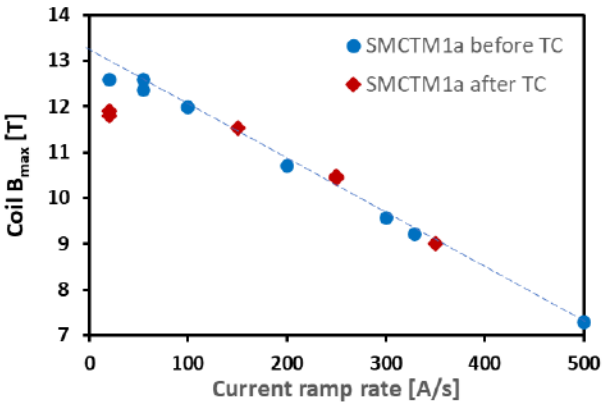

Figure 5: SMCT1 coil B_{max} vs. current ramp rate at 1.9 K measured in SMCTM1a configuration. The data at 20 A/s indicate that magnet training was not completed.

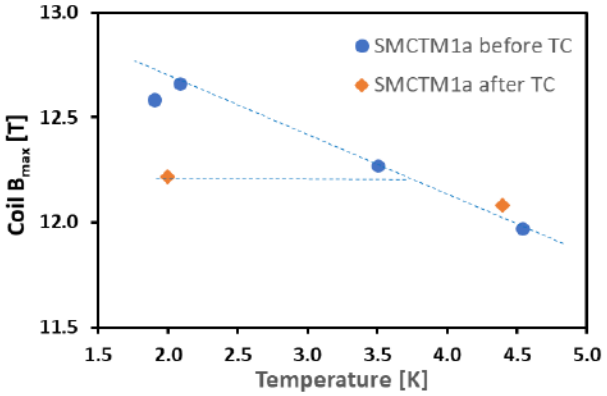

Figure 6: SMCT1 coil B_{max} vs. temperature measured in SMCTM1a configuration. The data show that magnet training at ~2 K before and after TC was not completed.

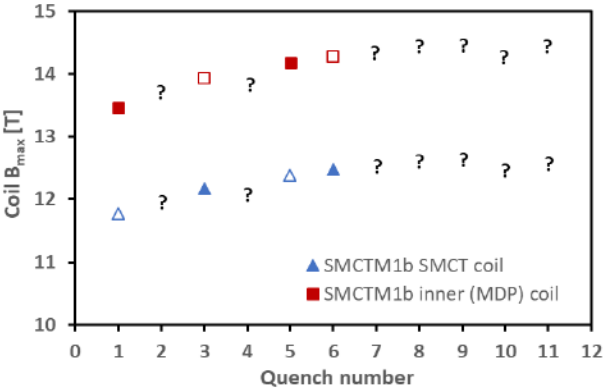

Figure 7: SMCT1 and MDP coil B_{max} vs. quench number at 20 A/s measured in SMCTM1b configuration at 1.9 K. Quenches with voltage spikes detected in both coils are shown by question marks.

The temperature dependence of the SMCT1 coil B_{max} measured before TC shows that the maximum field in the coil linearly reduced from 12.7 to 12.0 T which corresponds to 90% of the conductor limit at 4.5 K. The ~9% reduction of achieved coil B_{max} with respect to the SSL at both 1.9 K and 4.5 K could be due to conductor degradation during coil fabrication and mirror assembly. The causes are being analysed and will be improved in the next coils.

Consistency of coil B_{max} ramp rates above 150 A/s and B_{max} at ~4.5 K in SMCTM1a configuration before and after TC confirms that the coil has not degraded after TC.

SMCTM1b test

After warming up and reconfiguration of coil connection, SMCTM1b was cooled down and the test continued.

SMCT1 and MDP coil B_{max} vs. quench number during SMCTM1b training at 1.9 K is shown in Fig. 7. Coil quenches occurred in both coils, quench origin is shown by solid markers. The presence of current and voltage spikes in this test complicated identifying the quench origin. Quenches with voltage spikes detected in both coils are shown by question marks. The first quenches in SMCT1 coil occurred at coil B_{max} above 12 T which are higher than the quenches in SMCTM1a after TC. The magnet performance was limited due to large degradation of the inner coil. The maximum field reached in the SMCT and inner MDP coils at 1.9 K was 12.6 T and 14.5 T respectively.

CONCLUSION

The SMCT coil concept was proposed and is being studied at Fermilab for high-field and/or large-aperture accelerator magnets based on low-temperature and high-temperature superconductors. The SMCT coil structure allows reducing coil deformations under Lorentz forces and, thus, the high stresses in the coil, dangerous for coils made of brittle superconductors.

The first large-aperture Nb_3Sn SMCT1 dipole coil was designed and built at Fermilab to validate and study the SM coil concept. The SMCT1 coil was tested in two dipole mirror configurations. In the first test, after a relatively short training, the SMCTM1a mirror magnet with the SMCT1 coil powered individually, has reached a B_{max} in the coil of 12.7 T at 1.9 K and 12.0 T at 4.5 K which corresponds to ~90% of its SSL. After TC the magnet re-training started at 11.2 T showing some loss of its training memory. However, no conductor degradation was found after TC. The possible causes of magnet re-training are being studied and effort will be made to improve the situation in the next coils. In the four-layer SMCTM1b configuration, the B_{max} reached in the SMCT1 coil at 1.9 K was 12.6 T at the B_{max} in the inner MDP coil of 14.5 T. The SMCTM1b magnet performance was limited by the inner coil.

Successful demonstration of SMCT coil shows that this design approach open possibilities of large-aperture high-field dipole and quadrupole magnets for Muon Collider [9]-[11] and other applications such as 2nd IR for EIC [12].

ACKNOWLEDGMENTS

The authors thank V.V. Kashikhin for the coil magnetic optimization; J. Carmichael and J. Coghill for the end part design; A. Rusy and J. Karambis for the technical support of this work; G. Chlachidze, S. Krave, D. Orris, S. Stoynev and technical staff of Fermilab's Magnet Test Facility for the help with magnet testing.

REFERENCES

[1] V.V. Kashikhin, I. Novitski, A.V. Zlobin, "Design studies and optimization of high-field Nb_3Sn dipole magnets for a future Very High Energy *pp* Collider," in *Proc. IPAC'17*, Copenhagen, Denmark, May 2017, pp. 3597-3599. doi:10.18429/JACoW-IPAC2017-WEPVA140

[2] A.V. Zlobin *et al.*, "Conceptual design of a 17 T Nb_3Sn accelerator dipole magnet," in *Proc. IPAC'18*, Vancouver, Canada, Apr.-May 2018, pp. 2742-2744. doi:10.18429/JACoW-IPAC2018-WEPML027

[3] I. Novitski *et al.*, "Development of a 120-mm Aperture Nb_3Sn Dipole Coil with Stress Management," *IEEE Trans. Appl. Supercond.*, vol. 32, no. 6, pp. 1–5, Sep. 2022. doi:10.1109/tasc.2022.3163062.

[4] I Novitski *et al.*, "Using Additive Manufacturing technologies in high-field accelerator magnet coils," FERMILAB-CONF-21-369-TD, 2021.

[5] E. Barzi *et al.*, "Development and Fabrication of Nb_3Sn Rutherford Cable for the 11 T DS Dipole Demonstration Model", *IEEE Trans. Appl. Supercond.*, vol. 22, no. 3, Art. no. 6000805, Jun. 2012. doi:10.1109/tasc.2011.2180869

[6] A.V. Zlobin *et al.*, "Development and Test of a Single-Aperture 11T Nb_3Sn Demonstrator Dipole for LHC Upgrades", *IEEE Trans. Appl. Supercond.*, vol. 23, no. 3, Art. no. 4000904, Jun.2013. doi:10.1109/tasc.2012.2236138

[7] A.V. Zlobin *et al.*, "Development and First Test of the 15 T Nb_3Sn Dipole Demonstrator MDPCT1", *IEEE Trans. Appl. Supercond.*, vol. 30, no. 4, pp 1-5, Jun. 2020. doi:10.1109/tasc.2020.2967686

[8] A.V. Zlobin *et al.*, "Reassembly and Test of High-Field Nb_3Sn Dipole Demonstrator MDPCT1", *IEEE Trans. Appl. Supercond.*, vol. 31, no. 5, pp. 1-5, Aug. 2021. doi:10.1109/tasc.2021.3057571

[9] V.V. Kashikhin et al., "Magnets for Interaction Regions of a 1.5×1.5 TeV Muon Collider", in *Proc. IPAC2012*, New Orleans, LA, USA, May 2012, paper THPPD035, pp. 3584-3586.

[10] V.V. Kashikhin *et al.*, "High-Field Combined Function Magnets for a 1.5×1.5 TeV MC Storage Ring", in *Proc. IPAC2012*, New Orleans, LA, USA, May 2012, paper THPPD036, pp.3587-3589.

[11] A.V. Zlobin *et al.*, "Storage Ring and Interaction Region Magnets for a μ+μ- Higgs Factory", in *Proc. NA-PAC'13*, Pasadena, CA, USA, Sep.-Oct. 2013, paper THPBA19, pp. 1271-1273.

[12] A.V. Zlobin *et al.*, "Feasibility Study of Large-aperture High-field Nb_3Sn Magnets for the 2nd EIC Interaction Region," in *Proc. IPAC'23*, Venice, Italy, May 2023, pp. 3716-3719. doi:10.18429/JACoW-IPAC2023-WEPM063